



ELSEVIER

Computer Aided Geometric Design 11 (1994) 391-410

COMPUTER
AIDED
GEOMETRIC
DESIGN

Filling polygonal holes with bicubic patches

John A. Gregory¹, Jianwei Zhou²

Department of Mathematics and Statistics, Brunel University, Uxbridge, UB8 3PH, UK

Received August 1991; revised June 1993

Abstract

Consider a bicubic rectangular patch complex which surrounds an n -sided hole in \mathbb{R}^3 . Then the problem of filling the hole with n bicubic rectangular patches is studied.

Keywords: Bicubic patch; Polygonal hole

1. Introduction

The problem of filling a polygonal hole, which occurs within a smooth parametric rectangular patch complex, is one which arises frequently in free-form surface modelling, for example, where a number of surfaces are to be blended together. Here, we consider the situation where the rectangular patch complex is composed of bicubic patches which form a C^1 surface about an n -sided hole. A method is proposed for filling the n -sided hole with bicubic rectangular patches such that the resulting patch complex is a C^1 surface.

The development of such a method is not new, for example Van Wijk (1986) gives a detailed study of such a technique, based on the use of a certain type of continuity constraint between the bicubic patches. However, Liu (1986), Liu and Hoschek (1989), and Peters (1989) have observed that a more general type of continuity constraint between polynomial patches is allowable, and it is the general continuity constraint condition which we are going to study in this paper.

¹ Dr. John A. Gregory died very suddenly and unexpectedly on the evening of Friday 26 March 1993. The co-author, Dr. Jianwei Zhou, would like to dedicate his work in this paper to the memory of his mentor and friend.

² Present affiliation: Department of Mechanical Engineering, University College London, Torrington Place, London WC1E 7JE, UK.

The bicubic method proposed here is that reported on in the tutorial paper (Gregory et al., 1990), where a variety of techniques for filling n -sided holes is surveyed. In the case $n = 3$, a closed form solution is produced. In the case of an n -sided hole, $n > 4$, solutions are produced by constraining certain of the boundary data coefficients, and by further splitting.

A Hermite representation of the bicubic patches will be assumed in the development of the theory, rather than the use of Bernstein–Bézier representation. This will allow us to impose C^1 continuity constraints on the rectangular patch complex surrounding the hole through the choice of common Hermite data coefficients and this leads to some simplification of the analysis.

In Section 2 we give a precise statement of the polygonal hole problem and introduce the basic continuity constraint conditions for filling the hole with bicubic patches. A detailed analysis of the continuity constraints is given in Section 3. This analysis is used in the development of the schemes for filling an n -sided hole in the cases $n = 3$ and $n > 4$ described in Section 4.

2. Description of the problem

2.1. Bicubic patches

The bicubic Hermite patch $\mathbf{p} : [0, 1]^2 \rightarrow \mathbb{R}^3$ is defined by

$$\mathbf{p}(u, v) = \begin{pmatrix} H_0(u) \\ H_1(u) \\ H_2(u) \\ H_3(u) \end{pmatrix}^T \begin{pmatrix} \mathbf{P}_{0,0} & \mathbf{P}_{0,1} & \mathbf{P}_{0,0}^v & \mathbf{P}_{0,1}^v \\ \mathbf{P}_{1,0} & \mathbf{P}_{1,1} & \mathbf{P}_{1,0}^v & \mathbf{P}_{1,1}^v \\ \mathbf{P}_{0,0}^u & \mathbf{P}_{0,1}^u & \mathbf{P}_{0,0}^{u,v} & \mathbf{P}_{0,1}^{u,v} \\ \mathbf{P}_{1,0}^u & \mathbf{P}_{1,1}^u & \mathbf{P}_{1,0}^{u,v} & \mathbf{P}_{1,1}^{u,v} \end{pmatrix} \begin{pmatrix} H_0(v) \\ H_1(v) \\ H_2(v) \\ H_3(v) \end{pmatrix}, \quad (2.1)$$

where

$$\begin{aligned} H_1(u) &= H_0(1-u) = -2u^3 + 3u^2, \\ H_3(u) &= -H_2(1-u) = u^3 - u^2. \end{aligned} \quad (2.2)$$

This Hermite representation of a bicubic patch has the interpolation property that, at the vertices (i, j) of $[0, 1]^2$,

$$(\mathbf{p}(i, j) \ \mathbf{p}_u(i, j) \ \mathbf{p}_v(i, j) \ \mathbf{p}_{u,v}(i, j)) = (\mathbf{P}_{i,j} \ \mathbf{P}_{i,j}^u \ \mathbf{P}_{i,j}^v \ \mathbf{P}_{i,j}^{u,v}), \quad i, j = 0, 1, \quad (2.3)$$

where $\mathbf{p}_u = \partial \mathbf{p} / \partial u$, $\mathbf{p}_v = \partial \mathbf{p} / \partial v$, $\mathbf{p}_{u,v} = \partial^2 \mathbf{p} / \partial u \partial v$, see Fig. 1. Furthermore, along the edges, the boundary curves $\mathbf{p}(u, 0)$, $\mathbf{p}(u, 1)$, $\mathbf{p}(0, v)$, $\mathbf{p}(1, v)$ and the cross boundary tangent vector derivatives $\mathbf{p}_v(u, 0)$, $\mathbf{p}_v(u, 1)$, $\mathbf{p}_u(0, v)$, $\mathbf{p}_u(1, v)$ are univariate cubic Hermite functions. These univariate functions are determined completely by the vertex values on those edges. Thus two patches \mathbf{p} and \mathbf{q} can be joined with position and tangent plane continuity by appropriate identification of vertex data along their common boundary. This

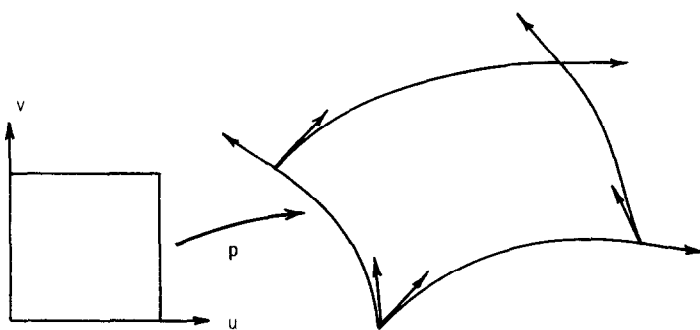


Fig. 1. Bicubic Hermite patch.

situation is well known in the construction of surface complexes of rectangular patches, where at each vertex there are four edges meeting (a “regular” vertex). The patch complex can then be considered as a single map from a parametric domain, subdivided by a regular rectangular mesh. We now wish to consider the more complex situation of filling an n -sided hole with n bicubic patches, where there are now n edges meeting at a vertex, $n \neq 4$ (a “non-regular” vertex).

2.2. The polygonal hole problem

Consider the situation shown in Fig. 2 of an n -sided “hole” in \mathbb{R}^3 surrounded by rectangular bicubic patches with regular vertices. The patches are assumed to form a C^1 surface around the hole, this being achieved by having identical vertex interpolation data along common edges. The j th “boundary edge” of the hole, $j = 0, \dots, n - 1$, is defined by two adjoining bicubic patches, as shown in the figure. (This includes the situation of having one bicubic patch adjacent to the boundary edge as a degenerate case.)

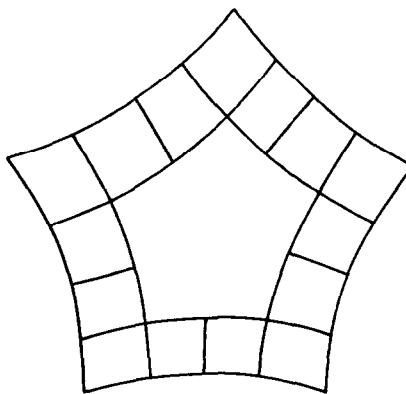


Fig. 2. The polygonal hole problem.

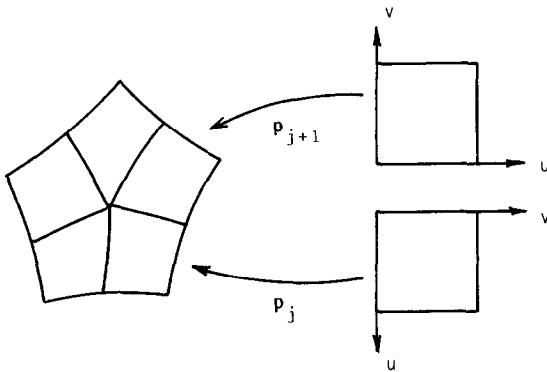


Fig. 3. Filling the hole with rectangular patches.

We wish to fill the n -sided hole with n bicubic patches $\mathbf{p}_j : [0, 1]^2 \rightarrow \mathbb{R}^3$, $j = 0, \dots, n - 1$, which meet at a non-regular n -vertex and which adjoin the regular rectangular patch complex with parameterizations as shown in Fig. 3. Thus $\mathbf{p}_j(s, 1)$ and $\mathbf{p}_{j+1}(1, s)$ must match the j th boundary edge of the hole and $\partial_{0,1}\mathbf{p}_j(s, 1)$ and $\partial_{1,0}\mathbf{p}_{j+1}(1, s)$ must match the cross boundary tangent. Hence the vertex data of the patches \mathbf{p}_j and \mathbf{p}_{j+1} along the j th edge of the hole are identified with those of the adjoining bicubic patches. In particular, we denote

$$\begin{aligned} \mathbf{B}_j &= \mathbf{p}_j(0, 1) = \mathbf{p}_{j+1}(1, 0), \\ \mathbf{B}_j^u &= -\partial_{1,0}\mathbf{p}_j(0, 1) = \partial_{0,1}\mathbf{p}_{j+1}(1, 0), \\ \mathbf{B}_j^v &= -\partial_{0,1}\mathbf{p}_j(0, 1) = -\partial_{1,0}\mathbf{p}_{j+1}(1, 0), \\ \mathbf{B}_j^{u,v} &= \partial_{1,1}\mathbf{p}_j(0, 1) = -\partial_{1,1}\mathbf{p}_{j+1}(1, 0), \quad j = 0, \dots, n - 1. \end{aligned} \quad (2.4)$$

Similarly, the vertex data at the corners of the polygonal hole are also defined by the adjoining rectangular patches, but will not be required explicitly in the analysis. This leaves us with the degrees of freedom at the central n -vertex, where we denote

$$\begin{aligned} \mathbf{Q} &= \mathbf{p}_j(0, 0), \\ \mathbf{Q}_j &= \partial_{0,1}\mathbf{p}_j(0, 0) = \partial_{1,0}\mathbf{p}_{j+1}(0, 0), \\ \mathbf{Q}_{j-1,j} &= \partial_{1,1}\mathbf{p}_j(0, 0), \quad j = 0, \dots, n - 1 \end{aligned} \quad (2.5)$$

2.3. The basic continuity constraint equations

The choice of the bicubic Hermite data for the patches \mathbf{p}_j , $j = 0, \dots, n - 1$, of the previous subsection, means that these patches have C^1 joins with the bicubic patches surrounding the hole. We are thus concerned with achieving a C^1 surface across the “interior edges” about the n -vertex \mathbf{Q} . It is well known that this involves constraint equations of the form

$$\mathbf{p}_{j+1}(s, 0) - \mathbf{p}_j(0, s) = \mathbf{0}, \quad (2.6)$$

and

$$\begin{aligned} \alpha_j(s)\partial_{1,0}\mathbf{p}_j(0, s) + \beta_j(s)\partial_{0,1}\mathbf{p}_j(0, s) + \gamma_j(s)\partial_{0,1}\mathbf{p}_{j+1}(s, 0) &= \mathbf{0}, \\ j &= 0, \dots, n-1, \end{aligned} \quad (2.7)$$

where

$$\alpha_j(s)\gamma_j(s) > 0. \quad (2.8)$$

The constraint (2.6) is that for C^0 continuity and in our case is automatically satisfied since $\mathbf{p}_{j+1}(s, 0)$ and $\mathbf{p}_j(0, s)$ are univariate Hermite functions which share common interpolation data, see (2.4) and (2.5). The constraint (2.7) is that for C^1 , that is tangent plane, continuity and has become known as the “geometric” GC^1 constraint in the CAGD literature. The condition (2.8) is imposed to avoid cusp like joins between the patches.

In (Liu, 1986), (Liu and Hoschek, 1989) and (Peters, 1989), it is observed that, in the case of bicubic patches, where $\partial_{1,0}\mathbf{p}_j(0, s)$ and $\partial_{0,1}\mathbf{p}_{j+1}(s, 0)$ are cubic polynomials and $\partial_{0,1}\mathbf{p}_j(0, s)$ is quadratic, the scalar factors $\alpha_j(s)$ and $\gamma_j(s)$ can be at most quintic polynomials, and $\beta_j(s)$ sextic. We consider this situation in detail in the following section. In particular, we are concerned with analyzing the constraints (2.7) around the n -vertex.

3. A study of the continuity constraints

3.1. C^1 continuity at the n -vertex

We first consider the constraint equation (2.7) at the n -vertex \mathbf{Q} , where $s = 0$. Thus with $s = 0$ in (2.7) and (2.8) we obtain

$$\alpha_j(0)\mathbf{Q}_{j-1} + \beta_j(0)\mathbf{Q}_j + \gamma_j(0)\mathbf{Q}_{j+1} = \mathbf{0}, \quad j = 0, \dots, n-1, \quad (3.1)$$

where

$$\alpha_j(0)\gamma_j(0) > 0. \quad (3.2)$$

It is required that

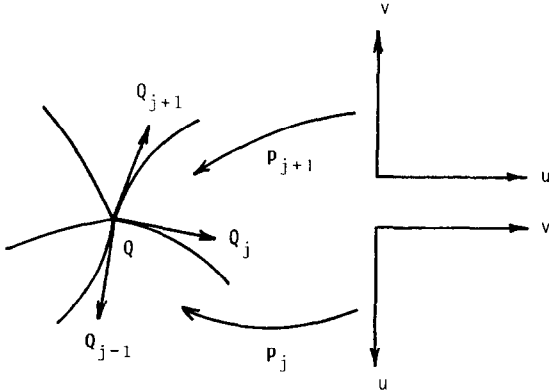
$$\dim \text{span}\{\mathbf{Q}_0, \mathbf{Q}_1, \dots, \mathbf{Q}_{n-1}\} = 2 \quad (3.3)$$

so that the vectors \mathbf{Q}_j lie in a common tangent plane at \mathbf{Q} , see Fig. 4. We also assume, without loss of generality, that

$$\alpha_j(0) = 1, \quad j = 0, \dots, n-1. \quad (3.4)$$

To proceed with the analysis, we now typically consider the “symmetric” equal coefficient case, where

$$\beta_j(0) = \beta_0 \quad \text{and} \quad \gamma_j(0) = \gamma_0 > 0, \quad j = 0, \dots, n-1. \quad (3.5)$$

Fig. 4. The n -vertex situation.

The vertex constraints (3.1) are thus

$$\mathbf{Q}_{j-1} + \beta_0 \mathbf{Q}_j + \gamma_0 \mathbf{Q}_{j+1} = \mathbf{0}, \quad j = 0, \dots, n-1. \quad (3.6)$$

Furthermore, the following geometrical constraints on the vectors \mathbf{Q}_j , $j = 0, \dots, n-1$, are imposed: Let θ_j denote the angle from \mathbf{Q}_j to \mathbf{Q}_{j+1} , $j = 0, \dots, n-1$, (all measured under a common orientation). Then it is assumed that

$$\sum_{j=0}^{n-1} \theta_j = 2\pi \quad \text{and} \quad \theta_j > 0, \quad j = 0, \dots, n-1. \quad (3.7)$$

These assumptions imply that the vectors \mathbf{Q}_j , $j = 0, \dots, n-1$, form a non-overlapping star in the tangent plane at the central vertex \mathbf{Q} and that

$$\mathbf{Q}_j \neq \mathbf{Q}_l \quad \text{for } j \neq l, 0 \leq j, l \leq n-1, \quad (3.8)$$

see Fig. 4. We now have the following:

Proposition 3.1. *There exists $\{\mathbf{Q}_j\}_{j=0}^{n-1}$ satisfying the vertex constraints (3.6) and the non-overlapping star conditions (3.7) if and only if*

$$\beta_0 = -2 \cos(2\pi/n) \quad \text{and} \quad \gamma_0 = 1. \quad (3.9)$$

Furthermore,

$$\begin{aligned} \mathbf{Q}_j &= [\sin(2j\pi/n)\mathbf{Q}_1 - \sin(2(j-1)\pi/n)\mathbf{Q}_0] / \sin(2\pi/n), \\ j &= 0, \dots, n-1. \end{aligned} \quad (3.10)$$

Proof. The constraints (3.6) define a homogeneous, constant coefficient, difference equation giving

$$\mathbf{Q}_j = \frac{\lambda^j - \mu^j}{\lambda - \mu} \mathbf{Q}_1 - \frac{\mu\lambda^j - \lambda\mu^j}{\lambda - \mu} \mathbf{Q}_0, \quad j = 0, \dots, n-1, \quad (3.11)$$

for $\lambda \neq \mu$ and

$$\mathbf{Q}_j = j\lambda^{j-1}\mathbf{Q}_1 - (j-1)\lambda^j\mathbf{Q}_0, \quad j = 0, \dots, n-1, \quad (3.12)$$

for $\lambda = \mu$, where λ and μ are the roots of the auxiliary equation

$$1 + \beta_0 x + \gamma_0 x^2 = 0. \quad (3.13)$$

The vectors \mathbf{Q}_j , $j = 0, \dots, n-1$, should also satisfy the periodicity requirement

$$\mathbf{Q}_{j+n} = \mathbf{Q}_j, \quad j = 0, \dots, n-1. \quad (3.14)$$

Thus, the solution (3.12) is inappropriate because for \mathbf{Q}_n given by (3.12), the equation $\mathbf{Q}_n = \mathbf{Q}_0$ and the linear independence of \mathbf{Q}_0 and \mathbf{Q}_1 imply that

$$n\lambda^{n-1} = 0 \quad \text{and} \quad 1 + (n-1)\lambda^n = 0,$$

which are inconsistent. Now imposing the periodicity conditions (3.14) on the solution given by (3.11), we obtain $\lambda^n = \mu^n = 1$, which implies that

$$\lambda = e^{i2k\pi/n}, \quad \mu = e^{i2l\pi/n}, \quad 0 \leq k, l \leq n-1.$$

The requirement that $\lambda\mu$ and $\lambda + \mu$ be real, see (3.13), then leads to the restriction that

$$\lambda = e^{i2k\pi/n}, \quad \mu = e^{-i2k\pi/n}, \quad 1 \leq k < n/2,$$

after further analysis. Hence

$$\mathbf{Q}_j = \frac{\sin(j\psi_k)}{\sin(\psi_k)}\mathbf{Q}_1 - \frac{\sin((j-1)\psi_k)}{\sin(\psi_k)}\mathbf{Q}_0, \quad j = 0, \dots, n-1, \quad (3.15)$$

where

$$\psi_k = 2k\pi/n \in (0, \pi), \quad 1 \leq k < n/2,$$

and thus $\sin \psi_k > 0$. We want to show that k can only be 1. If $2 \leq k < n/2$, then $n > 4$ and there exists some integer l , with $2 < l < n-1$, such that $(l-1)k < n \leq lk$. If $n = lk$ then (3.15) gives $\mathbf{Q}_l = \mathbf{Q}_0$ which contradicts (3.8). Thus $(l-1)k < n < lk$, that is, $0 < lk - n < k$. Therefore, we have

$$l\psi_k = 2\pi + 2(lk - n)\pi/n \in (2\pi, 3\pi)$$

and

$$(l-1)\psi_k = 2\pi + 2(lk - n - k)\pi/n \in (\pi, 2\pi).$$

Hence

$$\sin(l\psi_k) > 0 \quad \text{and} \quad \sin((l-1)\psi_k) < 0.$$

Thus, from (3.15), \mathbf{Q}_l lies between \mathbf{Q}_0 and \mathbf{Q}_1 since it is a positive linear combination of \mathbf{Q}_0 and \mathbf{Q}_1 . This violates (3.7). Hence $k = 1$ is the only value acceptable in (3.15) which completes the proof. \square

Remark 3.2. A corollary to Proposition 3.1, which follows from (3.3), is that the rank of the cyclic coefficient matrix defined in (3.6) is $n - 2$.

Remark 3.3. The solution (3.10) can be expressed as

$$\mathbf{Q}_j = \cos(2j\pi/n)\mathbf{X} + \sin(2j\pi/n)\mathbf{Y}, \quad j = 0, \dots, n-1, \quad (3.16)$$

and

$$\mathbf{X} = \mathbf{Q}_0 \quad \text{and} \quad \mathbf{Y} = \csc(2\pi/n)\mathbf{Q}_1 - \cot(2\pi/n)\mathbf{Q}_0. \quad (3.17)$$

Thus there is an affine map under which the vectors \mathbf{Q}_j , $j = 0, \dots, n-1$, form a regular star.

3.2. C^1 continuity across the interior edges

We now study the continuity constraint equations (2.7) in the symmetric case where $\alpha_j(s)$, $\beta_j(s)$ and $\gamma_j(s)$ are independent of j . Thus (2.7) is written as

$$\alpha(s)\partial_{10}\mathbf{p}_j(0, s) + \beta(s)\partial_{01}\mathbf{p}_j(0, s) + \gamma(s)\partial_{01}\mathbf{p}_{j+1}(s, 0) = \mathbf{0}, \quad (3.18)$$

where we denote the scalar polynomials by

$$\alpha(s) = \sum_i \alpha_i s^i, \quad \beta(s) = \sum_i \beta_i s^i, \quad \gamma(s) = \sum_i \gamma_i s^i. \quad (3.19)$$

(The suffix notation in (3.19) should not be confused with that for $\alpha_j(0)$, $\beta_j(0)$ and $\gamma_j(0)$ in Section 3.1.) It has been referenced in Section 2 that α , γ can be at most quintic polynomials and β can be at most sextic, but for our purpose here it is easier to assume the general power series forms (3.19), where the higher order coefficients are zero. Our purpose is to analyse the solvability of (3.18) assuming that the polygonal hole data (2.4) are given a priori. We shall see that in the case $n = 3$ a solution of (3.18) is possible but that for $n \geq 5$ a solution is not possible, in general. In Section 4 we will consider a specific solution for the case $n = 3$. In the case $n \geq 5$ we will obtain a solution of (3.18), where some of the polygonal hole data (2.4) are determined a posteriori.

Equating coefficients in (3.18) gives

$$\begin{aligned} \mathbf{E}_{i,j} := & 6(\beta_{i-1} - \beta_{i-2})(\mathbf{B}_j - \mathbf{Q}) + (\alpha_i - 3\alpha_{i-2} + 2\alpha_{i-3})\mathbf{Q}_{j-1} \\ & + (\beta_i - 4\beta_{i-1} + 3\beta_{i-2})\mathbf{Q}_j + (\gamma_i - 3\gamma_{i-2} + 2\gamma_{i-3})\mathbf{Q}_{j+1} \\ & - (3\alpha_{i-2} - 2\alpha_{i-3} - 3\gamma_{i-2} + 2\gamma_{i-3})\mathbf{B}_j^u + (2\beta_{i-1} - 3\beta_{i-2})\mathbf{B}_j^v \\ & + (\alpha_{i-1} - 2\alpha_{i-2} + \alpha_{i-3})\mathbf{Q}_{j-1,j} + (\gamma_{i-1} - 2\gamma_{i-2} + \gamma_{i-3})\mathbf{Q}_{j,j+1} \\ & - (\alpha_{i-2} - \alpha_{i-3} - \gamma_{i-2} + \gamma_{i-3})\mathbf{B}_j^{uv} = \mathbf{0}, \quad i = 0, 1, \dots, \end{aligned} \quad (3.20)$$

where any coefficients with negative suffices are interpreted as zero. For $i = 0$, (3.20) gives the vertex constraints

$$\alpha_0 \mathbf{Q}_{j-1} + \beta_0 \mathbf{Q}_j + \gamma_0 \mathbf{Q}_{j+1} = \mathbf{0}, \quad j = 0, \dots, n-1, \quad (3.21)$$

which from Section 3.1 has the solution

$$\alpha_0 = 1 = \gamma_0, \quad \beta_0 = -2 \cos(2\pi/n). \quad (3.22)$$

For the purpose of analysis, we consider the transformed equations

$$\sum_{i=0}^{\infty} i^k \mathbf{E}_{i,j} = \mathbf{0}, \quad j = 0, \dots, n-1, \quad (3.23)$$

for $k = 0, 1, \dots$, where $\mathbf{E}_{i,j}$ is defined by (3.20). The following proposition presents a negative result.

Proposition 3.4. *For $n \geq 5$, the constraints (3.23) are solvable for arbitrary boundary data $\{\mathbf{B}_j, \mathbf{B}_j^u, \mathbf{B}_j^v\}_{j=0}^{n-1}$ if and only if*

$$\alpha(s) = \beta(s) = \gamma(s) \equiv 0. \quad (3.24)$$

Proof. We first consider the constraint

$$\sum_i \mathbf{E}_{i,j} \equiv - \sum_i (\alpha_i - \gamma_i) \mathbf{B}_j^u - \sum_i \beta_i \mathbf{B}_j^v = \mathbf{0}. \quad (3.25)$$

Thus,

$$\sum_i (\alpha_i - \gamma_i) = 0 = \sum_i \beta_i, \quad (3.26)$$

since the two tangent vectors \mathbf{B}_j^u and \mathbf{B}_j^v at the boundary vertex \mathbf{B}_j must be linearly independent. We then consider $\sum i \mathbf{E}_{i,j} = \mathbf{0}$ and obtain

$$\sum i (\alpha_i - \gamma_i) = 0 = \sum i \beta_i. \quad (3.27)$$

Now we proceed by induction, assuming that the constraints (3.23) are solvable for $k = 0, \dots, m$, $m \geq 1$, if and only if

$$\sum i^l \alpha_i = 0, \quad l = 0, \dots, m-2, \quad (3.28)$$

$$\sum i^l \beta_i = 0 = \sum i^l (\alpha_i - \gamma_i), \quad l = 0, \dots, m. \quad (3.29)$$

(In the case $m = 1$, (3.28) is void.) Then for $k = m+1$, (3.23) gives

$$6\beta_0 \sigma_{1,m} \mathbf{Q}_j + \sigma_{2,m} \mathbf{B}_j^u + \sigma_{3,m} \mathbf{B}_j^v = 2\sigma_{1,m} (\mathbf{Q}_{j-1,j} + \mathbf{Q}_{j,j+1}), \quad (3.30)$$

where

$$\begin{aligned} \sigma_{1,m} &= \binom{m+1}{2} \sum_i i^{m-1} \alpha_i, & \sigma_{2,m} &= \sum_i i^{m+1} (\alpha_i - \gamma_i), \\ \sigma_{3,m} &= \sum_i i^{m+1} \beta_i. \end{aligned} \quad (3.31)$$

By using (3.30) itself, (3.20) for $i = 1$ and the vertex constraints

$$\mathbf{Q}_{j-1} + \beta_0 \mathbf{Q}_j + \mathbf{Q}_{j+1} = \mathbf{0}, \quad j = 0, \dots, n-1,$$

to eliminate the terms $\{\mathbf{Q}_{j-1,j} + \mathbf{Q}_{j,j+1}\}$, $\{\mathbf{Q}_j\}$ and \mathbf{Q} , we derive

$$\begin{aligned} & 12\beta_0\sigma_{1,m}[(\mathbf{B}_{l-1} - \mathbf{B}_l) + \beta_0(\mathbf{B}_l - \mathbf{B}_{l+1}) + (\mathbf{B}_{l+1} - \mathbf{B}_{l+2})] \\ & + \sigma_{2,m}[(\mathbf{B}_{l-1}^u - \mathbf{B}_l^u) + \beta_0(\mathbf{B}_l^u - \mathbf{B}_{l+1}^u) + (\mathbf{B}_{l+1}^u - \mathbf{B}_{l+2}^u)] \\ & + (\sigma_{3,m} + 4\beta_0\sigma_{1,m})[(\mathbf{B}_{l-1}^v - \mathbf{B}_l^v) + \beta_0(\mathbf{B}_l^v - \mathbf{B}_{l+1}^v) + (\mathbf{B}_{l+1}^v - \mathbf{B}_{l+2}^v)] = \mathbf{0}. \end{aligned} \quad (3.32)$$

For $n \geq 5$ the three vectors in (3.32) will, in general, be linearly independent and $\beta_0 \neq 0$ for $n \neq 4$, see (3.9). Hence

$$\sigma_{1,m} = \sigma_{2,m} = \sigma_{3,m} = 0$$

which completes the inductive step. \square

Remark 3.5. From Proposition 3.4 we conclude that the continuity constraints are not solvable in general for $n \geq 5$ with arbitrarily given Hermite boundary data. For $n = 3$, however, equation (3.32) is satisfied identically since $\beta_0 = 1$.

4. Methods for filling the n -sided hole

In this section we consider particular solutions to the continuity constraint equations (3.18) which result practical methods for filling n -sided holes with bicubic patches. As was observed in the previous section, we find it appropriate to distinguish between the case $n = 3$ and the case $n \geq 5$. We first, however, consider the choice of the scalar coefficients $\alpha(s)$, $\beta(s)$ and $\gamma(s)$ in the constraints (3.18).

4.1. A particular continuity constraint

From (3.9) we have

$$\alpha(0) = 1 = \gamma(0) \quad \text{and} \quad \beta(0) = -2 \cos(2\pi/n). \quad (4.1)$$

Also, from (3.26) and (3.27) we see that

$$\beta(1) = \beta'(1) = 0 \quad \text{and} \quad \alpha(1) - \gamma(1) = \alpha'(1) - \gamma'(1) = 0. \quad (4.2)$$

This latter condition reflects the fact that \mathbf{B}_j^u and \mathbf{B}_j^v must be linearly independent for a regular surface. Equations (4.1) and (4.2) are necessary conditions that the scalar functions $\alpha(s)$, $\beta(s)$ and $\gamma(s)$ must satisfy. The analysis made in Section 3.2 shows that, in general, no advantage is likely to be gained from imposing higher degrees on these scalar functions. Thus, for simplicity, we

now choose the minimum degree scalar polynomials consistent with (4.1) and (4.2), namely,

$$\alpha(s) = \gamma(s) = 1 \quad \text{and} \quad \beta(s) = \beta_0(1-s)^2, \quad (4.3)$$

where

$$\beta_0 = -2 \cos(2\pi/n). \quad (4.4)$$

Substituting in (3.18) then gives the quartic polynomial equation

$$\Phi_j(s) := \partial_{10}\mathbf{p}_j(0,s) + \beta_0(1-s)^2\partial_{01}\mathbf{p}_j(0,s) + \partial_{01}\mathbf{p}_{j+1}(s,0) = \mathbf{0}, \quad (4.5)$$

where, by the choice (4.3),

$$\Phi_j(0) = \Phi_j(1) = \Phi'_j(1) = \mathbf{0}.$$

Thus, we only require two additional constraints in order that (4.5) is satisfied. We take these as

$$\Phi'_j(0) = \Phi''_j(0) = \mathbf{0},$$

which give the two constraints

$$\begin{aligned} 6\beta_0(\mathbf{B}_j - \mathbf{Q}) - 6\beta_0\mathbf{Q}_j + 2\beta_0\mathbf{B}_j^v + \mathbf{Q}_{j-1,j} + \mathbf{Q}_{j,j+1} &= \mathbf{0}, \\ -18\beta_0(\mathbf{B}_j - \mathbf{Q}) + 15\beta_0\mathbf{Q}_j - 7\beta_0\mathbf{B}_j^v - 2(\mathbf{Q}_{j-1,j} + \mathbf{Q}_{j,j+1}) &= \mathbf{0}, \\ j &= 0, \dots, n-1, \end{aligned} \quad (4.6)$$

see equations (3.20) for $i = 1$ and 2. Thus, for the choice of the scalar functions (4.3), the constraints (4.6), together with the vertex constraint

$$\mathbf{Q}_{j-1} + \beta_0\mathbf{Q}_j + \mathbf{Q}_{j+1} = \mathbf{0}, \quad j = 1, \dots, n-1, \quad (4.7)$$

are necessary and sufficient conditions for a GC^1 join between the patches \mathbf{p}_j and \mathbf{p}_{j+1} .

4.2. Solution for the case $n = 3$

In the case $n = 3$ we have $\beta_0 = 1$ and the constraints (4.6) and (4.7) then give

$$\begin{aligned} 6(\mathbf{B}_j - \mathbf{Q}) - 6\mathbf{Q}_j + 2\mathbf{B}_j^v &= -(\mathbf{Q}_{j-1,j} + \mathbf{Q}_{j,j+1}), \\ 2(\mathbf{B}_j - \mathbf{Q}) - \mathbf{Q}_j + \mathbf{B}_j^v &= \mathbf{0}, \\ \mathbf{Q}_0 + \mathbf{Q}_1 + \mathbf{Q}_2 &= \mathbf{0}, \quad j = 0, 1, 2. \end{aligned} \quad (4.8)$$

We thus have

Proposition 4.1. *A symmetric solution to the triangular hole problem, for given Hermite boundary data, is*

$$\begin{aligned}\mathbf{Q} &= \frac{1}{3}\mathbf{V} + \frac{1}{6}\mathbf{W}, \\ \mathbf{Q}_j &= 2\mathbf{B}_j + \mathbf{B}_j^v - \frac{2}{3}\mathbf{V} - \frac{1}{3}\mathbf{W}, \\ \mathbf{Q}_{j-1,j+1} &= -6\mathbf{B}_j - 4\mathbf{B}_j^v + 2\mathbf{V} + \frac{3}{2}\mathbf{W}, \quad j = 0, 1, 2,\end{aligned}\tag{4.9}$$

where

$$\mathbf{V} = \mathbf{B}_0 + \mathbf{B}_1 + \mathbf{B}_2, \quad \mathbf{W} = \mathbf{B}_0^v + \mathbf{B}_1^v + \mathbf{B}_2^v.\tag{4.10}$$

Here, the value of \mathbf{Q} in (4.9) follows by summing the second equation in (4.8) over j and this second equation is then solved for \mathbf{Q}_j . The value of $\mathbf{Q}_{j-1,j+1}$ is now given by the solution of the cyclic system defined by the first equation in (4.8) for $j = 0, 1, 2$.

Remark 4.2. The above analysis shows that the continuity constraints can be satisfied in the case $n = 3$, that is, there is a solution for arbitrarily given Hermite boundary data around the triangular hole.

Figs. 5–7 show a model example of a triangular hole being filled with three bicubic patches with the interior vertex data determined by (4.9). It can be seen that a satisfactory tangent planar continuous surface is obtained by this method.

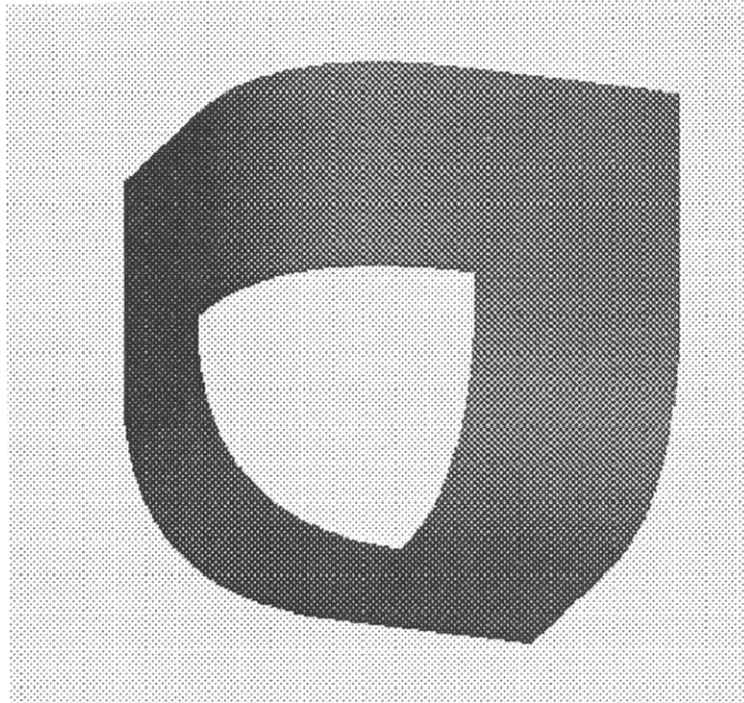


Fig. 5.

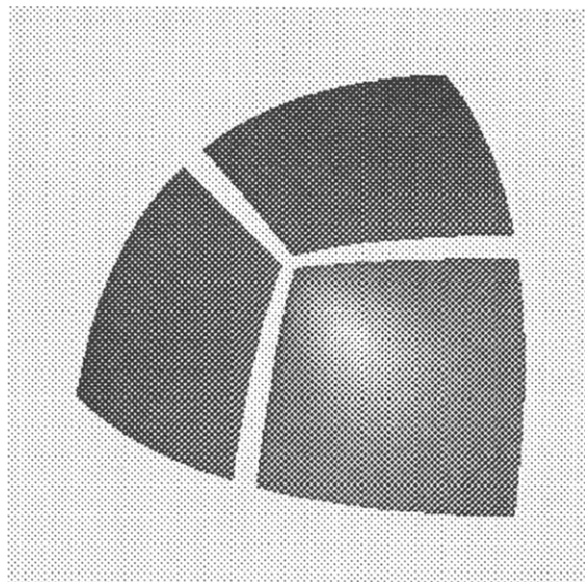


Fig. 6.

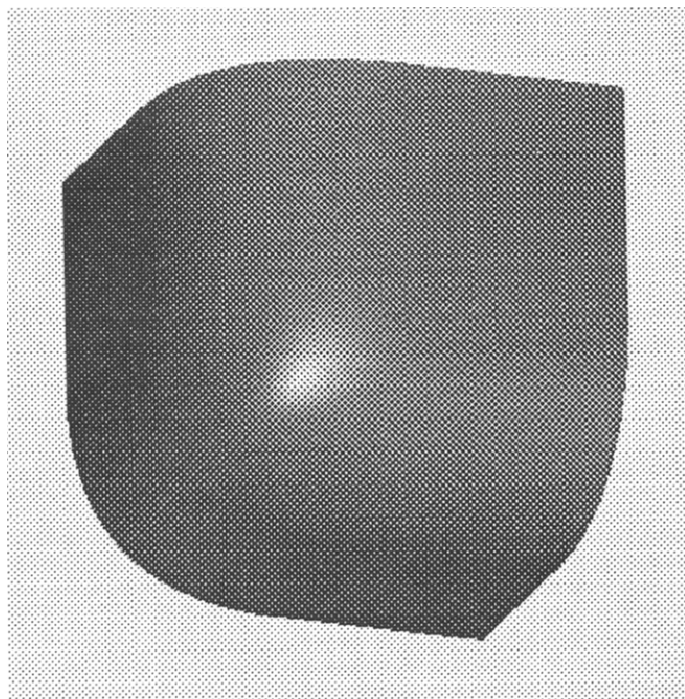


Fig. 7.

4.3. Solution for general n

The analysis of Section 3 shows that it is generally impossible to solve the n -sided polygonal hole problem with n bicubic Hermite patches in terms of arbitrarily given Hermite boundary data. In this case we may consider allowing the Hermite boundary data parameters $\{\mathbf{B}_j, \mathbf{B}_j^v\}$, $j = 0, \dots, n - 1$, to be additional degrees of freedom.

These parameters, together with the n -vertex parameters \mathbf{Q} and $\{\mathbf{Q}_j, \mathbf{Q}_{j,j+1}\}$, $j = 0, \dots, n - 1$, are then constrained by the underdetermined system of equations (4.6) and (4.7). There are then many possible ways of seeking appropriate solutions to this underdetermined system. For simplicity here, we observe that if the n -vertex parameters are given subject to the vertex constraint (4.7), then

$$\begin{aligned} \mathbf{B}_j &= \mathbf{Q} + 2\mathbf{Q}_j - \frac{1}{2\beta_0}(\mathbf{Q}_{j-1,j} + \mathbf{Q}_{j,j+1}), \\ \mathbf{B}_j^v &= -3\mathbf{Q}_j + \frac{1}{\beta_0}(\mathbf{Q}_{j-1,j} + \mathbf{Q}_{j,j+1}), \quad j = 0, \dots, n - 1, \end{aligned} \quad (4.11)$$

provides a solution to the problem. However, Fig. 9 shows that this simple technique of perturbing some of the boundary data can lead to undesirable “bumps” being introduced into the tangent plane continuous surface. Here the pentagonal hole of Fig. 8 has been filled with five bicubic patches, where the

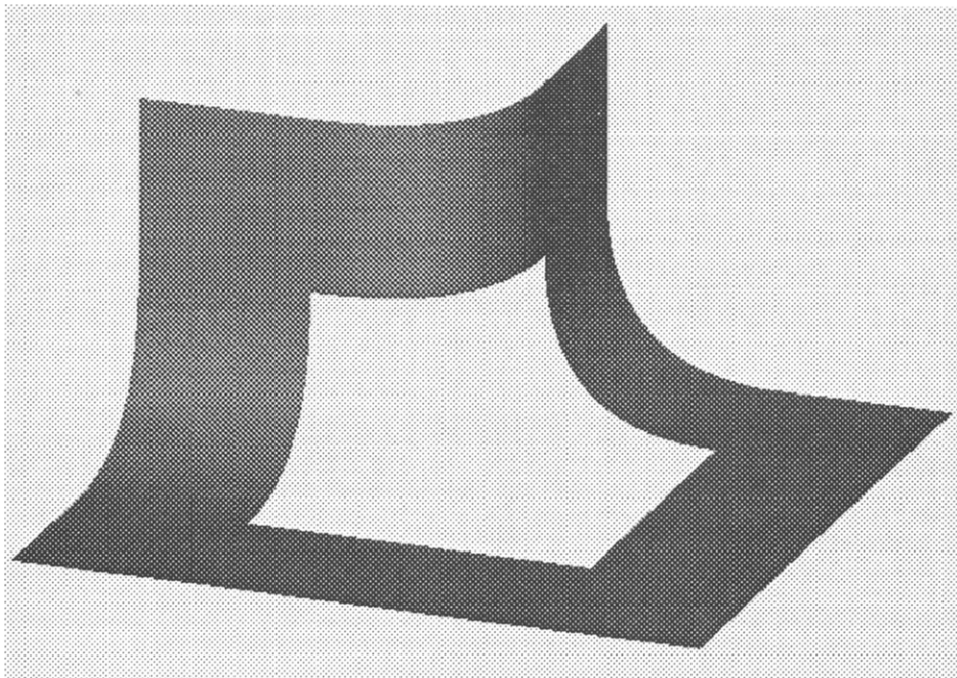


Fig. 8.

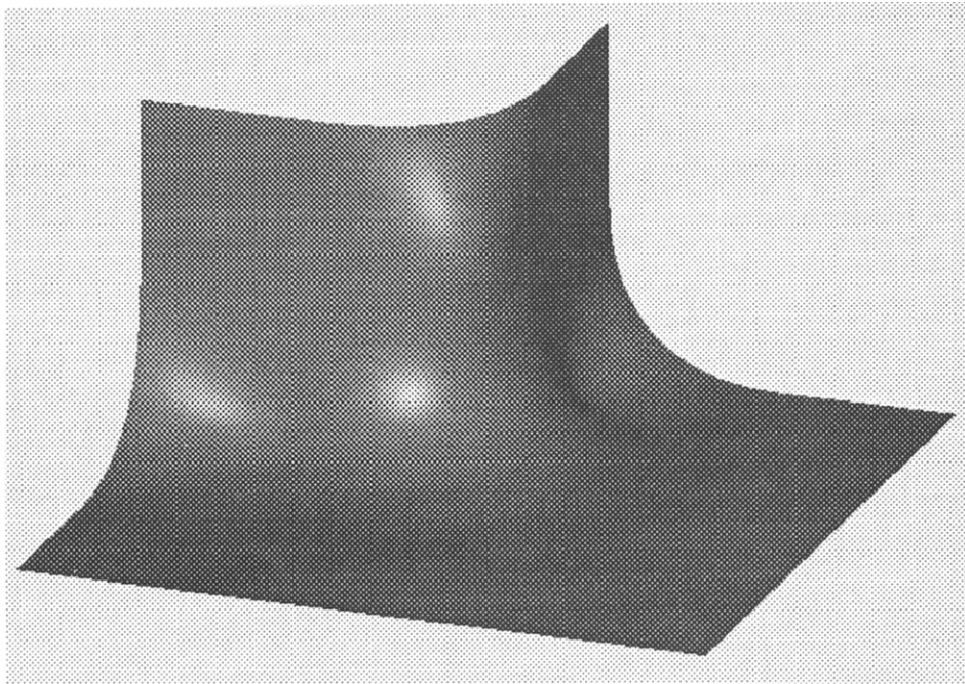


Fig. 9.

interior vertex data has been determined by an averaging process (in fact by (4.22) and one similar to (4.25)) and the boundary data has been perturbed to satisfy (4.11).

In order to avoid such bumpiness and to exactly match the given boundary Hermite data, we need to have more degrees of freedom. This can be achieved simply by further partitioning the hole with an additional layer of bicubic patches adjacent to the boundary. In practice, however, it results in too many extra degrees of freedom to be determined because each of the n rectangular patches used to fill the original hole is now split into four bicubic subpatches. We thus consider a constrained form of bicubic subpatch splitting through the introduction of double-cubic basis functions.

The additional double-cubic basis functions are defined as

$$h_0(u) = \begin{cases} 12u^2 - 16u^3, & u < \frac{1}{2}, \\ 12(1-u)^2 - 16(1-u)^3, & u \geq \frac{1}{2}, \end{cases} \quad (4.12)$$

and

$$h_1(u) = \begin{cases} (4u-2)u^2, & u < \frac{1}{2}, \\ (4u-2)(1-u)^2, & u \geq \frac{1}{2}. \end{cases} \quad (4.13)$$

It is easy to see that both $h_0(u)$ and $h_1(u)$ are C^1 functions and satisfy the cardinal conditions

$$h_k^{(i)}(u) = \delta_{u,1/2}\delta_{i,k}, \quad u = 0, \frac{1}{2}, 1, \quad i = 0, 1, \quad k = 0, 1. \quad (4.14)$$

The rectangular patches are then defined as

$$\begin{aligned} \mathbf{q}_j(u, v) &= \mathbf{p}_j(u, v) + (h_0(u) \ h_1(u)) \begin{pmatrix} \mathbf{C}_{j-1} & \mathbf{E}_{j-1} \\ \mathbf{D}_{j-1} & \mathbf{F}_{j-1} \end{pmatrix} \begin{pmatrix} H_0(v) \\ H_2(v) \end{pmatrix} \\ &\quad + (h_0(v) \ h_1(v)) \begin{pmatrix} \mathbf{C}_j & \mathbf{E}_j \\ \mathbf{D}_j & \mathbf{F}_j \end{pmatrix} \begin{pmatrix} H_0(u) \\ H_2(u) \end{pmatrix} \end{aligned} \quad (4.15)$$

where $\mathbf{p}_j(u, v)$, $j = 0, \dots, n - 1$, are the bicubic Hermite patches defined in Section 2 and

$$\begin{aligned} \mathbf{E}_j &= -\frac{1}{2}[\partial_{10}\mathbf{p}_j(0, \frac{1}{2}) + \partial_{01}\mathbf{p}_{j+1}(\frac{1}{2}, 0)], \\ \mathbf{F}_j &= -\frac{1}{2}[\partial_{11}\mathbf{p}_j(0, \frac{1}{2}) + \partial_{11}\mathbf{p}_{j+1}(\frac{1}{2}, 0)], \quad j = 0, \dots, n - 1. \end{aligned} \quad (4.16)$$

On the boundary of the hole, \mathbf{q}_j and \mathbf{p}_j match in position and the first order derivatives. The rectangular patch \mathbf{q}_j consists of four subpatches, each being a bicubic patch. Subpatches

$$\hat{\mathbf{p}}_j(u, v) = \mathbf{q}_j(u/2, v/2), \quad j = 0, \dots, n - 1,$$

cover the interior hole created by the partition and all the other subpatches form a C^1 surface around this interior hole.

We now apply the simple technique for filling polygonal holes, described in the beginning of this subsection, to the interior hole. It should be noted that the n rectangular patches defined by (4.15) will form a tangent plane continuous surface, as the result of this application.

In terms of the values of the subpatches $\hat{\mathbf{p}}_j$, $j = 0, \dots, n - 1$, the perturbation equations (4.11) are rewritten as

$$\begin{aligned} \hat{\mathbf{p}}_j(0, 1) &= \hat{\mathbf{p}}_j(0, 0) + 2\partial_{0,1}\hat{\mathbf{p}}_j(0, 0) - \frac{1}{2\beta_0}[\partial_{1,1}\hat{\mathbf{p}}_j(0, 0) + \partial_{1,1}\hat{\mathbf{p}}_{j+1}(0, 0)], \\ -\partial_{0,1}\hat{\mathbf{p}}_j(0, 1) &= -3\partial_{0,1}\hat{\mathbf{p}}_j(0, 0) + \frac{1}{\beta_0}[\partial_{1,1}\hat{\mathbf{p}}_j(0, 0) + \partial_{1,1}\hat{\mathbf{p}}_{j+1}(0, 0)], \\ j &= 0, \dots, n - 1, \end{aligned} \quad (4.17)$$

which are then expanded to give

$$\begin{aligned} \mathbf{C}_j &= \frac{1}{2}(\mathbf{Q} - \mathbf{B}_j) - \frac{1}{8}\mathbf{B}_j^v + \frac{7}{8}\mathbf{Q}_j - \frac{1}{8\beta_0}(\mathbf{Q}_{j-1,j} + \mathbf{Q}_{j,j+1}), \\ \mathbf{D}_j &= \frac{3}{2}(\mathbf{Q} - \mathbf{B}_j) - \frac{1}{4}\mathbf{B}_j^v + \frac{13}{4}\mathbf{Q}_j - \frac{1}{2\beta_0}(\mathbf{Q}_{j-1,j} + \mathbf{Q}_{j,j+1}), \\ j &= 0, \dots, n - 1. \end{aligned} \quad (4.18)$$

Equations (4.16) and (4.18) show that the extra degrees of freedom introduced by the splitting are determined in terms of the given boundary data $\{\mathbf{B}_j, \mathbf{B}_j^u, \mathbf{B}_j^v, \mathbf{B}_j^{uv}\}$ and the unknown central vertex data $\{\mathbf{Q}, \mathbf{Q}_j, \mathbf{Q}_{j-1,j}\}$.

We may also use (4.18) to determine the central vertex data. Equations (4.18) give

$$16\mathbf{C}_j - 4\mathbf{D}_j = 2(\mathbf{Q} - \mathbf{B}_j) - \mathbf{B}_j^v + \mathbf{Q}_j, \quad j = 0, \dots, n-1, \quad (4.19)$$

and

$$24\mathbf{C}_j - 4\mathbf{D}_j = 6(\mathbf{Q} - \mathbf{B}_j) - 2\mathbf{B}_j^v + 8\mathbf{Q}_j - \frac{1}{\beta_0}(\mathbf{Q}_{j-1,j} + \mathbf{Q}_{j,j+1}), \\ j = 0, \dots, n-1. \quad (4.20)$$

It is easily observed that the discontinuity in the second derivatives along the interior edges is caused by non-zero \mathbf{C}_j and \mathbf{D}_j . Thus, we wish to minimize the right hand side of (4.19) and (4.20), and hence to improve the smoothness of the resulting surface. Using (3.16), the Euclidean norm of the right hand side of (4.19) is expressed as

$$\left(\sum_{j=0}^{n-1} \left\| 2(\mathbf{Q} - \mathbf{B}_j) + \mathbf{X} \cos(2j\pi/n) + \mathbf{Y} \sin(2j\pi/n) - \mathbf{B}_j^v \right\|_2^2 \right)^{1/2}, \quad (4.21)$$

which is minimized to give

$$\mathbf{Q} = \frac{1}{n} \sum_{j=0}^{n-1} \mathbf{B}_j + \frac{1}{2n} \sum_{j=0}^{n-1} \mathbf{B}_j^v, \\ \mathbf{Q}_j = \frac{2}{n} \sum_{k=0}^{n-1} (2\mathbf{B}_k + \mathbf{B}_k^v) \cos(2(j-k)\pi/n), \quad j = 0, \dots, n-1. \quad (4.22)$$

Remark 4.3. In the case of a triangular hole, the central vertex data \mathbf{Q} and \mathbf{Q}_j , $j = 0, 1, 2$, expressed in (4.9) are reproduced by (4.22).

For the twists, we try to minimize the right hand side of (4.20). If n is odd, we can actually set the right hand side of (4.20) to zero, which gives

$$\mathbf{Q}_{j-1,j} + \mathbf{Q}_{j,j+1} = 2\mathbf{R}_j, \quad j = 0, \dots, n-1, \quad (4.23)$$

where

$$\mathbf{R}_j = 3\beta_0(\mathbf{Q} - \mathbf{B}_j) + 4\beta_0\mathbf{Q}_j - \beta_0\mathbf{B}_j^v. \quad (4.24)$$

Consequently, we derive the following formulae

$$\mathbf{Q}_{-1,0} = \sum_{i=0}^{n-1} (-1)^i \mathbf{R}_i, \quad \mathbf{Q}_{j,j+1} = 2\mathbf{R}_j - \mathbf{Q}_{j-1,j}, \quad j = 0, \dots, n-2, \quad (4.25)$$

for calculating the twists.

If n is even, the coefficient matrix of (4.23) is singular, we alternatively solve the twists by minimizing

$$\sum_{j=0}^{n-1} \left\| (\mathbf{Q}_{j-1,j} + \mathbf{Q}_{j,j+1}) - 2\mathbf{R}_i \right\|_2^2$$

subject to

$$\sum_{j=0}^{n-1} (-1)^j (\mathbf{Q}_{j-1,j} + \mathbf{Q}_{j,j+1}) = \mathbf{0},$$

and obtain

$$\mathbf{Q}_{j-1,j} + \mathbf{Q}_{j,j+1} = 2\hat{\mathbf{R}}_j, \quad j = 0, \dots, n-2, \quad (4.26)$$

where

$$\hat{\mathbf{R}}_j = \mathbf{R}_j - \frac{(-1)^j}{n} \sum_{i=0}^{n-1} (-1)^i \mathbf{R}_i. \quad (4.27)$$

One of the twist vectors, $\mathbf{Q}_{-1,0}$ say, may be assigned arbitrarily. A particular value, however, can be derived by further minimizing

$$\sum_{j=0}^{n-1} \left\| \mathbf{Q}_{j,j+1} \right\|_2^2.$$

Therefore, in the case of even n , the twists can be calculated using

$$\begin{aligned} \mathbf{Q}_{-1,0} &= \frac{2}{n} \sum_{i=0}^{n-1} (-1)^i (n-i) \hat{\mathbf{R}}_i, \\ \mathbf{Q}_{j,j+1} &= 2\hat{\mathbf{R}}_j - \mathbf{Q}_{j-1,j}, \quad j = 0, \dots, n-2, \end{aligned} \quad (4.28)$$

We summarize the above in the following proposition

Proposition 4.4. *For a given set of boundary Hermite data $\{\mathbf{B}_j, \mathbf{B}_j^u, \mathbf{B}_j^v, \mathbf{B}_j^{uv}\}$, the rectangular patches \mathbf{q}_j , $j = 0, \dots, n-1$, with the vector coefficients calculated from (4.25) or (4.28), (4.22), (4.18) and (4.16), form a GC^1 fill to the n -sided hole.*

Fig. 10 shows the result of the pentagonal hole displayed in Fig. 8 being filled with the above splitting technique. A more detailed study of this technique can be found in (Zhou, 1991).

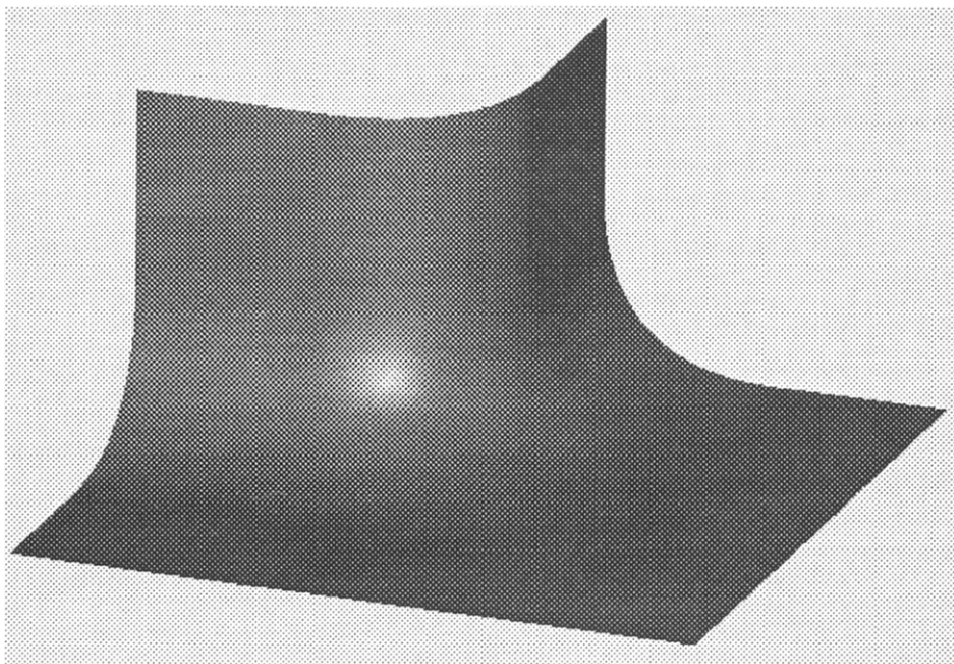


Fig. 10.

5. Conclusion

The main purpose of this paper has been to give a detailed analysis of the continuity equations which result from constraining n patches to meet at a non-regular n -vertex. For the case of a 3-vertex, it has been shown that there is a simple closed form solution of the constraint equations which enables a triangular hole to be filled with three bicubic patches. For the case of a general n -vertex, a closed form solution is not possible in general. However, the n -sided hole can still be filled, with n bicubic patches if some of the boundary vertex data are allowed to be perturbed, and with n rectangular patches, each consists of four bicubic subpatches. The theory and examples presented here demonstrate the existence of tangent plane continuous bicubic patch methods for filling polygonal holes.

Acknowledgements

We gratefully acknowledge the support of the ACME Directorate of the Science and Engineering Research Council, with grant GR/E 25092 and GR/F 80838, and of Siemens AG, with a Ph.D. studentship.

References

- Gregory, J.A., Lau, V.K.H. and Zhou, J. (1990), Smooth parametric surfaces and n -sided patches, in: W. Dahmen, M. Gasca and C.A. Micchelli, eds., *Computation of Curves and Surfaces*, NATO ASI Series, Kluwer Academic Publishers, Dordrecht, 457–498.
- Liu, D. (1986), A geometric condition for smoothness between adjacent Bézier surface patches, *Acta Math. Appl. Sinica* 9, 432–442.
- Liu, D. and Hoschek, J. (1989), GC^1 continuity conditions between adjacent rectangular and triangular Bézier surface patches, *Computer-Aided Design* 21, 194–200.
- Peters, J. (1989), Local interpolation of a cubic curve mesh by a piecewise biquartic C^1 surface without splitting, *Tech. Report 89-25*, University of Wisconsin.
- Van Wijk, J.J. (1986), Bicubic patches for approximating non-rectangular control-point meshes, *Computer Aided Geometric Design* 3, 1–13.
- Zhou, J. (1991), Geometric continuity and rectangular patch methods for surface modelling, Ph.D. thesis, Department of Mathematics and Statistics, Brunel University.